JOURNAL OF BACTERIOLOGY, Mar. 2009, p. 1463–1471 Vol. 191, No. 5
0021-9193/09/$08.00+0 doi:10.1128/JB.01583-08

Functional Differences of Two Distinct Catalases in *Mesorhizobium loti* MAFF303099 under Free-Living and Symbiotic Conditions▽

Masaki Hanyu,[1,2] Hanae Fujimoto,[1] Kouhei Tejima,[1] and Kazuhiko Saeki[1]*

Department of Biological Sciences, Faculty of Science, Nara Women's University, Nara 630-8506,[1] and Department of Biological Sciences, Graduate School of Science, Osaka University, Toyonaka, Osaka 560-0043,[2] Japan

Received 8 November 2008/Accepted 4 December 2008

Protection against reactive oxygen species (ROS) is important for legume-nodulating rhizobia during the establishment and maintenance of symbiosis, as well as under free-living conditions, because legume hosts might assail incoming microbes with ROS and because nitrogenase is extremely sensitive to ROS. We generated mutants of two potential catalase genes in *Mesorhizobium loti* MAFF303099 to investigate their physiological significance. Biochemical results indicated that genes with the locus tags mlr2101 and mlr6940 encoded a monofunctional catalase and a bifunctional catalase-peroxidase, respectively, that were named *katE* and *katG*. Under free-living conditions, the *katG* mutant demonstrated an extended generation time and elevated sensitivity to exogenous H_2O_2, whereas the *katE* mutant exhibited no generation time extension and only a slight increase in sensitivity to exogenous H_2O_2. However, the *katE* mutant showed a marked decrease in its survival rate during the stationary phase. With regard to symbiotic capacities with *Lotus japonicus*, the *katG* mutant was indistinguishable from the wild type; nevertheless, the mutants with disrupted *katE* formed nodules with decreased nitrogen fixation capacities (about 50 to 60%) compared to those formed by the wild type. These mutant phenotypes agreed with the expression profiles showing that transcription of *katG*, but not *katE*, was high during the exponential growth phase and that transcription levels of *katE* versus *sigA* were elevated during stationary phase and were approximately fourfold higher in bacteroids than mid-exponential-phase cells. Our results revealed functional separation of the two catalases, as well as the importance of KatE under conditions of strong growth limitation.

The genus *Rhizobium* comprises a group of soil bacteria that form nodules on the roots and stems of legume host plants for symbiotic nitrogen fixation. In the nodule, rhizobial cells differentiate into bacteroids that are able to reduce atmospheric nitrogen to ammonia. Bacteroids use respiratory oxidative phosphorylation to produce the ATP that is required for nitrogen fixation. This respiration process unavoidably generates reactive oxygen species (ROS), such as the superoxide radical (O_2^-) and hydrogen peroxide (H_2O_2). ROS can damage DNA, lipids, membranes, and proteins (for a review, see reference 13). In addition to the endogenous ROS, rhizobial cells might encounter exogenous ROS that are generated by host legume plants as defense measures against invading microorganisms (34, 38). For example, O_2^- and H_2O_2 were detected in infection threads, which are the passages through which rhizobia move into root cortex cells (34). Therefore, rhizobia must cope with ROS, not only of internal origin, but also of external origin, to establish symbiosis.

Among the ROS, H_2O_2 can penetrate biological membranes and react with intracellular free iron via the Fenton reaction to produce hydroxyl radicals ($HO^\bullet$), the most toxic ROS (for a review, see reference 13). To scavenge H_2O_2, aerobes have complex systems that consist of detoxification enzymes, redox mediators, and their regulatory components. H_2O_2 can be converted to O_2 and H_2O by catalases or, more correctly, hydroperoxidases (H_2O_2:H_2O_2 oxidoreductase; EC 1.11.1.6). Catalases are divided into heme-containing monofunctional catalases and bifunctional catalase-peroxidases, as well as manganese-containing catalases (for a review, see reference 6). The responses to oxidative stress have been most extensively studied in *Escherichia coli*, which synthesizes both a monofunctional catalase and a bifunctional catalase-peroxidase encoded by *katE* and *katG*, respectively (42, 45). These two *E. coli kat* genes are differentially controlled in regard to the growth phase and the cell's response to oxidative stress. *katG* expression is under the control of the transcriptional regulator OxyR, while *katE* requires the stationary-phase-specific sigma factor *rpoS* (32, 22, 40).

Among rhizobia, the number and enzymatic properties of catalases vary. For instance, *Bradyrhizobium japonicum* USDA110 and *Rhizobium etli* CFN42 each possess only one catalase or bifunctional catalase-peroxidase encoded by *katG*, which accompanies an *oxyR*-like gene (27, 44). By comparison, *Sinorhizobium meliloti* Rm1021 possesses as many as three catalases, two monofunctional catalases encoded by *katA* and *katC* and a bifunctional catalase-peroxidase encoded by *katB*; *katA* accompanies an *oxyR*-like gene (11, 14, 15, 39). In *B. japonicum* and *R. etli*, the *katG* mutation confers increased sensitivity to H_2O_2 under free-living conditions (27, 44). Notably, the *R. etli katG* mutant establishes nitrogen-fixing symbiosis with *Phaseolus vulgaris* that is as effective as that of the wild-type strain, although the mutant-induced bacteroids contain a number of proteins that are not found in the wild-type-induced bacteroids (44). In *S. meliloti*, a single mutation in any of the three *kat* genes does not apparently affect H_2O_2 sensitivity, but a *katA katC* double mutant and a *katB katC* double

* Corresponding author. Mailing address: Department of Biological Sciences, Faculty of Science, Nara Women's University, Nara 630-8506, Japan. Phone and fax: 81-742-20-3028. E-mail: ksaeki@cc.nara-wu.ac.jp.

▽ Published ahead of print on 12 December 2008.

TABLE 1. Bacterial strains and plasmids used in this study

Strains and plasmids	Relevant characteristics	Source or reference
Strains		
M. loti		
MAFF303099	Wild-type strain; Pm^r	17
ML2101D	MAFF303099 derivative; *katE* mutant	This study
ML6940DS	MAFF303099 derivative, *katG*::ΩSpc	This study
MLDKAT	ML2101D derivative, *katG*::ΩSpc	This study
E. coli		
DH10B	F^- *mcrA* Δ(*mrr-hsdRMS-mcrBC*) φ80d*lacZ* ΔM15 Δ*lacX74 deoR recA1 araD139* Δ(*ara leu*)*7697 galU galK* λ *rpsL endA1 nupG*	Invitrogen
HB101	*supE44* Δ(*mcrC-mrr*) *recA13 ara-14 proA2 lacY1 galK2 rpsL20 xyl-5 mtl-1 leuB6 thi-1*	33
StrataClone Solopack	F^- φ80d*lacZ* ΔM15 *endA recA tonA*	Stratagene
Plasmids		
pRK2013	RK2 derivative helper plasmid; Km^r	8
pKS800	Cloning vector; derivative of cosmid pLAFR1; Tc^r	10
c086	pKS800 containing MAFF303099 genome region coordinates 1703050–1725921; Tc^r	10
c279	pKS800 containing MAFF303099 genome region coordinates 5690329–5717656; Tc^r	10
pSC-B	Cloning vector; Amp^r	Stratagene
p2101SC-B	pSC-B derivative containing *katE*; Amp^r	This study
pHP45ΩSpc	ΩSpc; Amp^r	29
pKST001Rtr	pCR2.1 containing *aadA* flanked by FRTs; Amp^r Km^r Spc^r	Okabe and Saeki, unpublished
pSO012	pBBRI_MCS2 derivative; expression plasmid of *flp*; Km^r Tc^r	Maruya et al., unpublished
pK18mob	Mobilizable plasmid used for cloning and insertional disruption; Km^r	36
p2101Spc	p086r-mob derivative containing *katE*::FRT-*aadA*-FRT; Km^r Spc^r	This study
p6940ΩSpc	p279r-mob derivative containing *katG*::ΩSpc; Km^r Spc^r	This study
pKEZ01	pKS800 derivative containing *katE-lacZYA*; Tc^r	This study
pKGZ01	pKS800 derivative containing *katG-lacZYA*; Tc^r	This study
pEIS102	pRK415 derivative containing an artificial σ^{70} promoter; Tc^r	Mishima et al., unpublished
p2101EX	pEIS102 derivative containing *katE*; Tc^r	This study
P6940EX	pEIS102 derivative containing *katG*; Tc^r	This study

mutant are deficient in both nodule formation and nitrogen fixation (15, 39). By quantitative assay and native gel detection, a number of other rhizobia have been shown to contain two or three catalases, and enzyme contents vary both during growth and in response to the presence of H_2O_2 (26). These enzymatic variations suggest that different rhizobia adopt diverse strategies to utilize distinct set of catalases (and/or related enzymes) for both ex planta and in planta sustenance.

Mesorhizobium loti MAFF303099 is a microsymbiont of the model legume *Lotus japonicus*, which forms determinate-type nodules like *Glycine max* and *P. vulgaris* (12). The determinate-type nodules are spherical without persistent meristems and are distinct from the indeterminate-type nodules, which are cylindrical with persistent nodule meristems, which are formed by legumes such as the *Medicago* species (12). The annotation of the *M. loti* MAFF303099 genome indicates the presence of two catalase genes with the locus tags mlr2101 and mlr6940 on the main chromosome (17; http://www.kazusa.or.jp/rhizobase/index.html). The predicted amino acid sequence of Mlr2101 (702 residues) has similarity to those of monofunctional catalases, such as *S. meliloti* KatA (43% identity) and KatC (76%), as well as *E. coli* KatE (50%), while the sequence of Mlr6940 (756 residues) has similarity to those of bifunctional catalase-peroxidases, such as *S. meliloti* KatB (74%), *B. japonicum* KatG (76%), and *E. coli* KatG (61%). The assortment of catalases in *M. loti* MAFF303099 is unique among rhizobia. Hence, it is of great interest to determine whether the *M. loti* catalases play distinct roles under symbiotic conditions. Here, we report single and double gene disruptions and transcriptional analysis of the genes with locus tags mlr2101 and mlr6940 in *M. loti*.

MATERIALS AND METHODS

Bacterial strains and growth conditions. The bacterial strains and plasmids used are listed in Table 1. *E. coli* strains were grown in Luria-Bertani medium or Terrific broth (33) at 37°C. *M. loti* strains were routinely grown in tryptone-yeast extract (TY) medium (10) at 28°C. For aerobic growth, *M. loti* preculture was inoculated into 130 ml TY medium in a 500-ml flask to yield an optical density at 600 nm (OD_{600}) of approximately 0.02 and then shaken at 100 rpm in a personal Lt-10 incubator (Taitec, Japan). For semiaerobic growth, the preculture was inoculated into 300 ml TY medium in a 500-ml flask to an OD_{600} of ca. 0.05 and then shaken at 60 rpm. Ampicillin (Amp), kanamycin (Km), phosphomycin (Pm), spectinomycin (Spc), and tetracycline (Tc) were used at 100, 20, 100, 30, and 5 μg/ml, respectively, as needed.

Molecular genetic techniques. Molecular genetic procedures were performed according to previously described standard protocols (10, 33) unless otherwise stated. Conjugal transfer of plasmids from *E. coli* to *M. loti* was performed via triparental mating with helper *E. coli* HB101 harboring pRK2013 (8). Southern hybridization analysis was carried out using the appropriate PCR fragments labeled with digoxigenin-dUTP as previously described (31). End blunting of DNA fragments was performed with T4 DNA polymerase in the presence of deoxynucleoside triphosphate.

Cloning of the *M. loti* catalase genes. A 2,178-bp DNA fragment containing mlr2101 was PCR amplified using the primers 5′-CCACCCCAGAGATTGAG GAACCAG-3′ and 5′-GTTCGTGGTTCAGCCCAGCTTCAC-3′ from the cos-

mid c086. Another 2,387-bp fragment containing mlr6940 was amplified from c279 using the primers 5′-GCAATGCGGCCTAGTCTGGAATCG-3′ and 5′-GAAGGATTGATCGAACGCCTGAATGC-3′. These PCR products were cloned into pSC-B with a StrataClone Blunt PCR Cloning Kit (Stratagene) to obtain p2101SC and p6940SC, respectively. Plasmid p2101EX was constructed to express mlr2101 by subcloning an EcoRV-SmaI fragment from p2101SC into pEIS102, which possesses an artificial promoter (E. Mishima, E. Ishida, and K. Saeki, unpublished data). Similarly, subcloning a HindIII-SmaI fragment from p6940SC into pEIS102 generated p6940EX.

Deletion-insertion mutagenesis of the *M. loti* catalase genes. The 5,935-bp EcoRI fragment containing mlr2101 was excised from c086 and cloned into the suicide vector pK18mob (36) to make p86r-mob. After truncation by NheI digestion followed by self-ligation of p86r-mob, the 1,367-bp AscI-MfeI segment in the coding region of mlr2101 was replaced by a Flp recombinase recognition target FRT-*aadA*-FRT fragment that was composed of an Spc-resistant cassette with flanking FRT sequences excised from plasmid pKST001Rtr (S. Okabe and K. Saeki, unpublished data). The resultant plasmid, p2101Spc, was transferred into *M. loti* MAFF303099 for mlr2101 disruption. Mutants were first selected for Spc resistance and then screened for the loss of Km resistance. Mutants with the expected recombination were confirmed by PCR and Southern analysis. One of these mutants was named ML2101DS and was subjected to a procedure to remove the *aadA* gene flanked by FRT using an *flp* expression plasmid, pSO012 (J. Maruya, S. Okabe, and K. Saeki, unpublished data). The markerless mlr2101 mutant obtained was verified by Southern blot analysis and named ML2101D.

The 8,452-bp HindIII fragment containing mlr6940 was excised from cosmid c279 and subcloned into pK18mob. The resultant plasmid was digested with Acc65I and XbaI, blunted, and self-ligated to generate p279fT-mob. The 635-bp BamHI segment in the mlr6940 coding region in p279fT-mob was replaced by the ΩSpc cassette, which was excised from pHP45ΩSpc (29) after BamHI digestion. The resultant plasmid, p279ΩSpc, was used to construct the mlr6940 mutant ML6940DS and the mlr2101-mlr6940 double mutant MLDKAT through the screening and confirmation procedures described above.

Construction of *kat-lacZ* in-frame fusion plasmids. The plasmids used to monitor catalase gene expression were constructed by inserting a *lacZYA* fragment from pMCK2 (31) into the appropriate cosmid clones used in MAFF303099 genome sequencing (17). Plasmid pKEZ01 possessed a *katE-lacZ* gene to encode a chimeric protein that was the N-terminal 19 amino acids of mlr2101 product fused to *E. coli* β-galactosidase and the upstream genome fragment of approximately 4.9 kbp; likewise, pKGZ01 possessed a *katG-lacZ* gene to encode a protein with the N-terminal 80 amino acids of mlr6940 product and an upstream fragment of approximately 4.5 kbp.

Preparation of cell extracts. *M. loti* cells were quickly chilled, harvested centrifugally at 6,000 × *g* for 10 min, and washed once with 50 mM sodium phosphate buffer (pH 7.0). The cells were suspended in a fivefold volume (5 ml per wet weight of harvested cells) of the buffer containing 1.0 mM EDTA and 1.0 mM phenylmethylsulfonyl fluoride, a protease inhibitor, and immediately disrupted with a Mini-BeadBeater (Biospec Products Inc., Bartlesville, OK) twice for 20 s. The suspension was then centrifuged at 12,000 × *g* at 4°C for 10 min to remove cell debris. The resultant supernatant was used as cell extract.

H_2O_2 treatment of *M. loti* culture. To examine the catalase expression in response to exogenous H_2O_2, liquid culture was supplemented with H_2O_2 according to the method of Brown et al. (5). Briefly, *M. loti* cells were grown in TY medium to mid-exponential phase at an OD_{600} of around 0.4 under either aerobic or semiaerobic conditions and divided into two 40-ml aliquots. To one of the aliquots, 400 μl of 20 mM H_2O_2 was added five times at 10-min intervals, while H_2O was added to the other aliquot. Cells were harvested 20 min after the final addition and were used as either "H_2O_2-treated cells" or "control cells".

Detection and determination of enzyme activities. To visually detect catalase and peroxidase activities, cell extracts containing about 30 μg proteins were electrophoresed with 7% nondenaturing polyacrylamide gels. Catalase activity was visualized using previously established procedures (7), in which the electrophoresed catalase consumed H_2O_2 before the substrate was used to oxidize diaminobenzidine (DAB) with externally added horseradish peroxidase. The peroxidase activity was visualized by DAB oxidation in the presence of H_2O_2, as described previously (46).

The catalase activities of cell extracts were quantified by the decrease of absorbance at 240 nm that followed H_2O_2 decomposition in 50 mM sodium phosphate buffer (pH 7.0) (16). One unit of catalase was defined as the amount of enzyme that decomposed 1 μmol of H_2O_2 per minute under the assay conditions. β-Galactosidase activity was measured by Miller's method using *o*-nitrophenyl-β-D-galactoside as the substrate (25).

Growth profiling under aerobic conditions. Cell density was automatically recorded by measuring the OD_{660} every 10 min with a Bio-Photorecorder TN-1506 (Advantec, Tokyo, Japan). A preculture grown for 48 h was diluted into 4.5 ml TY medium to an OD_{660} of 0.02 in a specialized test tube and incubated at 28°C with shaking at 60 strokes per min.

H_2O_2 sensitivity assays. The killing effects of H_2O_2 on solid medium were investigated using an inhibition zone assay (28). Lawns of *M. loti* strains were formed by pouring approximately 1.2×10^8 cells grown overnight, suspended in 0.7% (wt/vol) agar at 45°C, onto TY agar plates (90 mm in diameter). Then, sterile Whatman AA discs (6 mm in diameter) containing 7 μl of 40 mM H_2O_2 were placed on each plate. Zones of growth inhibition were measured after incubation at 28°C for 4 days.

The threshold concentration of H_2O_2 that prevented proliferation was measured by batch culture experiments in which exponential- and stationary-phase *M. loti* cells were diluted to an OD_{600} of 0.05 in TY medium containing various concentrations of H_2O_2 and incubated at 28°C without shaking. After a 48-h incubation, cell densities were measured at OD_{630} using a Benchmark multiplate reader (Bio-Rad).

Evaluating cell survival. *M. loti* strains were aerobically grown in TY liquid medium. At the indicated times, samples were removed, and dilutions were plated on TY agar plates. Colonies were counted after 3 days of incubation at 28°C to determine the number of viable cells. We defined survival of 100% as corresponding to the viable-cell number determined at 35 h.

RNA isolation. Total-RNA samples from free-living *M. loti* cells were isolated using an acid-phenol method, as previously described (18), while samples from 9-week-old nodules were isolated with the RNeasy Plant Mini Kit (Qiagen). Before acid-phenol treatment, *M. loti* culture was mixed with 0.1 volume of 10% water-saturated phenol in ethanol, and then cells were collected by centrifugation at 5,000 × *g* for 5 min at 4°C. To remove residual DNA, each sample was treated with DNase I (TaKaRa, Kyoto, Japan) in the presence of RNase inhibitor according to the protocol supplied by the manufacturer. Total-RNA amounts were quantified spectrophotometrically.

qRT-PCR assay. Quantitative reverse transcription-PCR (qRT-PCR) was performed using the SuperScript III Platinum SYBR Green One-Step qRT-PCR Kit (Invitrogen). Each 20-μl reaction mixture consisted of 20 ng total RNA and 1 pmol specific primers. Real-time PCRs were run on a MiniOpticon thermal cycler (Bio-Rad). RNA samples isolated from at least three independent experiments were tested in triplicate for each condition. The primer pairs used were 5′-CACGACAATTTCTGGGATTTCATCTC-3′ and 5′-GAAAGTGTGGACGCCGAACC-3′ for *katE* and 5′-TCGGCAAAATCGGAGCAGTG-3′ and 5′-CATCGGGTCGGACAGAGAGG-3′ for *katG*. The transcript levels were normalized against that of *sigA* by the $2^{-\Delta\Delta}C^T$ method (23). The primers for *sigA* were from Uchiumi et al. (43).

Plant assays. Nodulation and plant growth were observed via the slant agar method as previously reported (10). Briefly, sterile 3-day-old *L. japonicus* B-129 seedlings were transplanted to a 1.5% agar slant containing nitrogen-free B&D medium (4) in 24- by 180-mm glass tubes and inoculated with approximately 10^6 bacteria. Each slant tube, with a plastic cover on the lower part, was incubated in a growth chamber (MLR-350H; Sanyo Ltd., Moriguchi, Japan) for a 16-h light/8-h dark cycle at 24°C with 70% humidity.

The nitrogen fixation capacities of nodules were quantified by acetylene reduction. Sterile 3-day old *L. japonicus* seedlings were grown for 1 week in plant boxes (four plants per box) (CUL-JAR300; Iwaki, Tokyo, Japan) containing sterile vermiculite; the seedlings were watered with nitrogen-free B&D medium (4) and inoculated with approximately 10^7 bacteria. After 5 weeks, whole roots from a plant box were cut and transferred to a 24- by 180-mm glass test tube. The tube was closed with a rubber double stopper, injected with 5 ml C_2H_2 gas, and incubated at 24°C in darkness. After 5 and 15 min of C_2H_2 injection, 500 μl of the gas phase was withdrawn to determine the C_2H_4 produced. Analysis was performed through a combination column of Polapak-Q (3 mm [inside diameter] by 1 m) and Polapak-N (3 mm [inside diameter] by 1 m) (Waters) at 120°C using a Shimadzu GC-14A gas chromatograph equipped with a flame ionization detector.

Histochemical detection of β-galactosidase activity. β-Galactosidase activities in roots and nodule cross sections were detected by previously described histochemical methods (20). Nodule cross sections were obtained by embedding harvested nodules in 5% agar, followed by sectioning them at 70 μm using a DTK-1000 microslicer (Dosaka, Kyoto, Japan). Samples were stained in 10 mM sodium phosphate buffer (pH 7.4) containing 2.7 mM KCl, 137 mM NaCl, and 0.8 mg/ml X-Gal (5-bromo-4-chloro-3-indolyl-β-D-galactopyranoside) for 3 to 6 h and observed with an Olympus BX-51 microscope.

Miscellaneous measurements. Absorbance was measured using a Shimadzu UV-1500 spectrophotometer or a NanoDrop spectrophotometer (NanoDrop Technologies, Wilmington, DE). The protein concentration was determined by

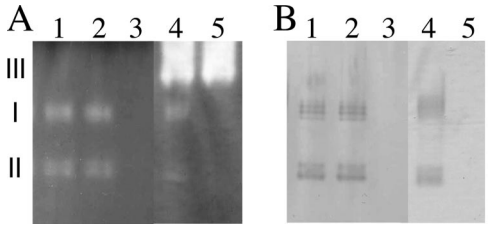

FIG. 1. Detection of catalase and peroxidase activities in extracts from *M. loti* wild-type and mutant cells. Extracts from cells grown in TY medium to an OD_{600} of 0.3 were electrophoresed through nondenaturing polyacrylamide gels. (A) Catalase activity was negatively visualized as colorless bands (I, II, and III) on an oxidized-DAB background due to H_2O_2 consumption by electrophoresed catalase in the presence of externally added horseradish peroxidase and H_2O_2. (B) Peroxidase activity was visualized as dark bands of oxidized DAB in the presence of H_2O_2, and 30 μg of protein was loaded per lane. The other conditions are described in Materials and Methods. The extracts were from MAFF303099 (lanes 1), ML2101D (lanes 2), ML6940DS (lanes 3), MAFF303099 harboring p2101EX (lanes 4), and ML6940DS harboring p2101EX (lanes 5).

the Bradford method using bovine serum albumin as a standard (3) with a protein assay kit (Bio-Rad).

RESULTS

Biochemical detection of two distinct catalases in *M. loti* MAFF303099. The annotation of the *M. loti* MAFF303099 genome predicted two potential catalase genes with the locus tags mlr2101 and mlr6940 (17). To address whether these predicted genes encoded functional catalases, we first performed activity stain analysis of the extracts of aerobically grown exponential-phase MAFF303099 cells. As expected, two achromatic bands were observed in the negative staining that detected general catalase activity by outcompeting H_2O_2-dependent DAB oxidation with exogenously added peroxidase (Fig. 1A, lane 1, bands I and II). However, two chromatic bands were also observed at the corresponding positions in the positive staining to detect peroxidase activity (Fig. 1B), indicating that there could be either two catalase-peroxidases or two forms of a catalase-peroxidase. To distinguish these possibilities, we constructed mutants of mlr2101 and mlr6940, named ML2101D and ML6940DS, respectively. The activity band patterns obtained with ML2101D were indistinguishable from those of the wild type (Fig. 1, lane 2), whereas no activity bands were observed with ML6940DS (Fig. 1, lane 3). These results revealed that both activity bands I and II resulted from a single bifunctional catalase-peroxidase encoded by mlr6940 and that this enzyme can have two different forms in native gel electrophoresis, as previously reported for the corresponding *E. coli* enzyme (24, 42). Expression of mlr2101 was also indicated to be below detection levels under the conditions employed. Further determination of H_2O_2 decomposition by cell extracts confirmed that the mlr6940 product was the primary contributor of total catalase activity in exponential-phase cells (Table 2).

Because the results did not confirm the presence of a functional mlr2101 product, we constructed an expression plasmid, p2101EX. Cell extracts from the MAFF303099 and ML6940DS strains, which harbor p2101EX, both exhibited a new achromatic band III in catalase negative staining but no additional band in peroxidase staining (Fig. 1, lanes 4 and 5). Preliminary sodium dodecyl sulfate-polyacrylamide gel analysis of a partially purified Mlr2101 sample indicated that the monomeric form was an approximately 75-kDa protein (data not shown). These results ascertained that the mlr2101 product was a monofunctional catalase of large-subunit subtype (6). Based on these results and the sequence similarities with *E. coli* enzymes, we designated mlr2101 and mlr6940 *katE* and *katG*, respectively.

Effects of catalase gene disruption on ex planta growth. During construction of the *katG* mutant ML6940DS, the mutant formed small, slowly growing colonies compared to the *katE* mutant, ML2101D. This observation could confirm the above-mentioned results by demonstrating that the *katG* product was the primary catalase during exponential growth. To further investigate the roles of *katE* and *katG*, we compared the growth capacities of the single mutants and a double mutant, MLDKAT. When cells were grown aerobically in liquid medium, the generation times of MAFF303099 and ML2101D were both approximately 4 h, while those of ML6940DS and MLDKAT were approximately 5.5 h. The maximal cell densities at early stationary phase attained by ML6940DS and MLDKAT were both about 90% of those attained by MAFF303099 and ML2101S. The slower growth phenotypes of the *katG* single and *katG katE* double mutants were complemented by transferring the cosmid, c279, containing *katG* (data not shown). The result suggested that KatG has an important, if not crucial, role in detoxification of internal H_2O_2 during aerobic growth and that the loss of *katG* cannot be compensated for by *katE*.

We assessed the effects of externally added H_2O_2 with an inhibition zone assay (Fig. 2). The results showed that ML6940DS and MLDKAT were both far more vulnerable to exogenous H_2O_2 than wild-type MAFF303099 and ML2101D. Transferring the cosmid c279 to ML6940DS decreased the size of the inhibition zone more than was seen in the wild-type cells. This slight overcomplementation could be caused by multiple copy numbers of c279 in the *M. loti* cells. In contrast, transferring another cosmid containing *katE*, termed c086, to ML2101D scarcely affected the zone of inhibition. To assess the threshold of exogenous H_2O_2 concentration that significantly prevented proliferation of each strain, we performed a batch culture experiment. These results revealed that proliferation of ML6940DS was completely arrested by the addition of 0.06 mM H_2O_2, but the proliferation of MAFF303099 and

TABLE 2. Catalase activities in *M. loti katE* and *katG* mutants and effects of exogenous H_2O_2 addition

Strain	Catalase activity (U/mg protein)[a]		Ratio[b]
	$-H_2O_2$	$+H_2O_2$	
MAFF303099	26.7 ± 2.0	45.8 ± 5.8	1.7
ML2101D	25.4 ± 0.6	42.2 ± 1.6	1.7
ML6940DS	0.0	0.0	

[a] Decomposition of H_2O_2 by cell extracts was determined by the decrease in the A_{240}. Cell extract preparation and addition of H_2O_2 were carried out as described in Materials and Methods. The activity values are the means of at least three experiments and are shown with standard deviations.

[b] Activity ratio of H_2O_2-treated versus mock treated.

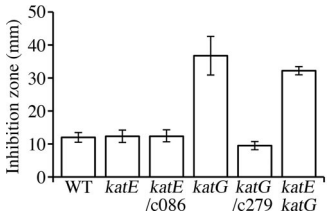

FIG. 2. Growth capacities of *M. loti* catalase mutants on solid medium in the presence of H_2O_2. Catalase mutants and their derivatives were subjected to an inhibition zone assay for H_2O_2 sensitivity, as described in Materials and Methods. The strains used were the wild type (WT), MAFF303099; *katE*, ML2101D; *katE*/c086, ML2101D harboring cosmid c086 that contained the *katE* gene; *katG*, ML6940DS; *katG*/c279, ML6940DS harboring cosmid c279 that contained the *katG* gene; and *katE katG*, MLDKAT. The data represent the means of at least four independent experiments, and the error bars indicate standard deviations.

ML2101D was not arrested by addition of less than 2 mM H_2O_2 (Fig. 3). These results suggested that KatG had a quasi-essential role in detoxifying exogenous H_2O_2 at approximately 0.06 mM or more under free-living conditions.

Effects of *katE* disruption on survival during stationary phase. While we were measuring the generation time of ML2101D, the lag time of the strain before exponential growth often fluctuated compared to MAFF303099. This observation led us to hypothesize that KatE might play a role during the stationary phase. To address this possibility, we assessed the survival rates of ML2101D and MAFF303099 during prolonged aerobic culturing in TY medium (Fig. 4). After inoculation of mid-exponential-phase cells into fresh TY medium by 100-fold dilution, the OD of both ML2101D and MAFF303099 reached a maximum at 48 h and maintained this density for at least 4 days. However, the viabilities of the cells as measured by CFU differed between the two strains. The *katE* mutant, ML2101D, started to lose viability shortly after reaching maximum cell numbers, whereas MAFF303099 maintained viability for 24 h or longer. This result indicated that *katE* contributed to the survival of stationary-phase cells.

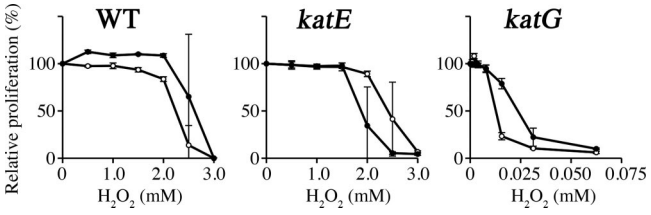

FIG. 3. Growth capacities of *M. loti* catalase mutants in liquid batch culture in the presence of H_2O_2. Catalase mutants were examined for growth capability in the presence of H_2O_2 in liquid medium. Cells grown to mid-exponetial and stationary phases (OD_{600} = 0.3 and 2.5, respectively) were inoculated in TY liquid medium that contained various concentrations of H_2O_2. The starting OD_{600} of each culture was fixed at 0.05, and the cells were grown at 28°C without shaking for 48 h. The cell density values were normalized to that obtained for a control culture without H_2O_2 addition. The strains used were the wild type (WT), MAFF303099; *katE*, ML2101D; and *katG*, ML6940DS. The open circles indicate that the inoculants were exponential-phase cells, while the closed circles indicate that the inoculants were stationary-phase cells. The data are the means of six experiments, and the error bars indicate standard deviations.

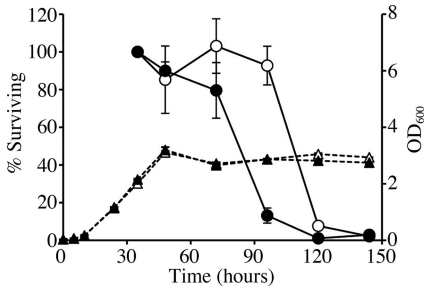

FIG. 4. Effects of *katE* mutation on survival after entering the stationary phase. Wild-type and *katE* mutant cells were examined for colony-forming capacity after the exponential phase. MAFF303099 and ML2101D cells were cultivated aerobically in TY medium at 28°C. Aliquots were taken at the indicated times and measured for both OD_{600} (triangles) and colony-forming capacity on TY agar medium (circles). Survival rates of 100% correspond to the colony-forming capacity determined at 35 h. The open symbols represent wild-type MAFF303099, while the closed symbols represent the *katE* mutant, ML2101D. The data are the means of three independent experiments. In each experiment, the colony-forming capacity was determined with at least four plates. The error bars indicate standard deviations.

Effects of catalase gene disruption on symbiosis. To investigate the effects of the catalase mutations on nodulation and nitrogen fixation, we inoculated *L. japonicus* seedlings with the mutants. During the 7-week observation period, plants inoculated with the three mutants were essentially indistinguishable in terms of leaf numbers (Fig. 5A) and plant heights (data not shown) from the plants inoculated with MAFF303099. However, plants inoculated with the *katE* mutants, ML2101D and MLDKAT, formed a larger number of nodules than those inoculated with MAFF303099 and ML6940DS 4 weeks after inoculation (Fig. 5B).

We then assessed nitrogenase activity by the acetylene reduction method. The activity values of ML2101D- and MLDKAT-induced nodules were approximately 55 to 60% of

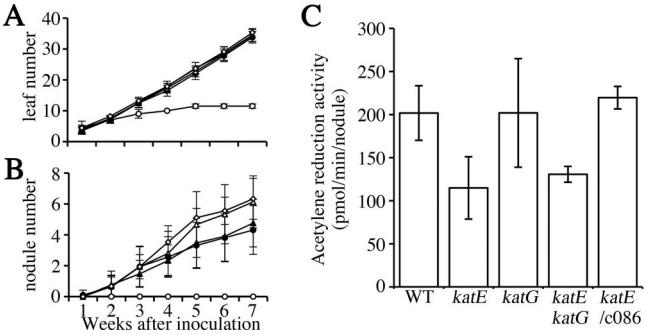

FIG. 5. Effects of catalase mutation on symbiotic capacities with *L. japonicus*. (A and B) Shown are leaf numbers (A) and nodule numbers (B) on *L. japonicus* plants inoculated with the examined *M. loti* strains. (C) C_2H_2 reduction activity per nodule measured at 5 weeks after inoculation. The cosmid clones c086 and c279 were used as complementation plasmids for *katE* and *katG* mutants, respectively. *L. japonicus* B-129 hosts were inoculated with wild-type (WT) MAFF303099 (closed circles), the *katE* mutant ML2101D (open triangles), the *katG* mutant ML6940DS (closed triangles), the *katE katG* double mutant MLDKAT (open diamonds), and the control, sterile water (open circles). The values are means obtained from at least 12 plants, and the error bars indicate standard deviations.

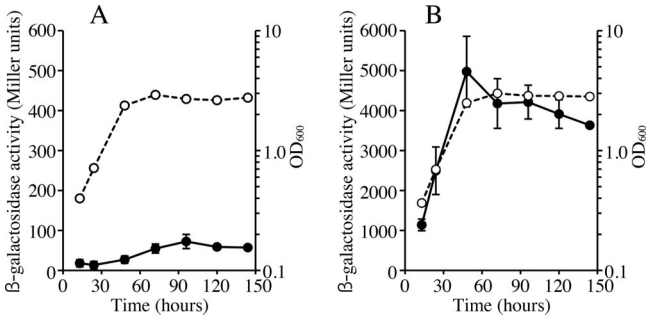

FIG. 6. Expression of *katE-lacZ* and *katG-lacZ* fusion genes in aerobic culture. Catalase gene expression was analyzed during growth stages by the expression of in-frame *lacZ* fusion genes, as described in Materials and Methods. β-Galactosidase activity and cell density were analyzed for MAFF303099 cells harboring pKEZ that contained the *katE-lacZ* genes (A) and pKGZ that contained the *katG-lacZ* gene (B). The open and closed circles indicate cell densities (OD_{600}) and β-galactosidase activities, respectively. The values are means of triplicate measurements in three independent experiments. The error bars indicate standard deviations.

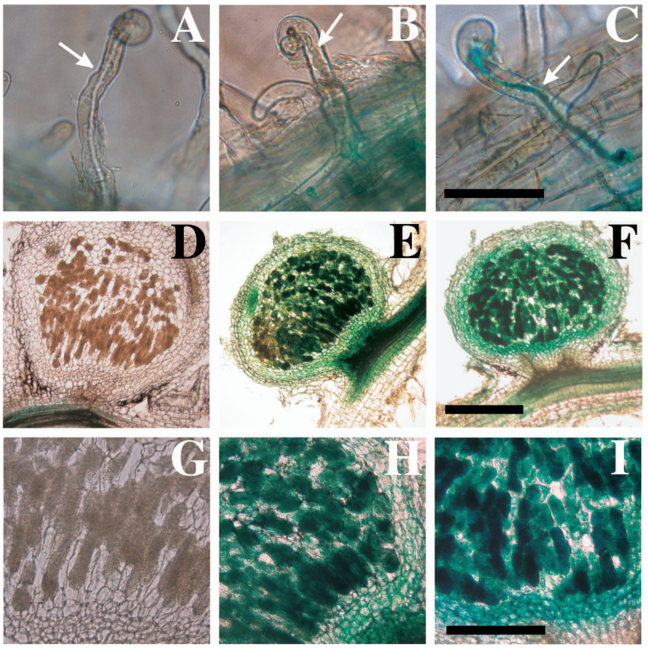

FIG. 7. Histochemical detection of catalase gene expression during *M. loti-L. japonicus* nodule development. β-Galactosidase activity was detected using X-Gal as a substrate. The photographs depict MAFF303099 (A, D, and G), MLKEZ01 (*katE-lacZYA*) (B, E, and H), and MLKGZ01 (*katG-lacZYA*) (C, F, and I). (A to C) Root hairs. (D to I) Sections of 7-week-old nodules. Scale bars = 100 μm (A to C), 200 μm (G to I), and 500 μm (D to F). The arrows indicate infection threads.

those of nodules induced by MAFF303099 and ML6940DS (Fig. 5C). Transferring the cosmid c086 containing *katE* to ML2101D complemented the decrease in nitrogenase activity (Fig. 5C), as well as the increase in nodule numbers (data not shown). These results indicated that KatE, but not KatG, optimized symbiotic nitrogen fixation with *L. japonicus*.

Expression of *katE* and *katG* under free-living conditions. The results of the catalase activity assays suggested that the expression levels of the two catalase genes are considerably different under free-living conditions. We constructed plasmids pKEZ01 and pKGZ01, containing in-frame *lacZ* fusions to *katE* and *katG*, respectively, which were transferred to MAFF303099, and determined β-galactosidase activities under aerobic growth conditions. The results indicated that *katG* expression increased during exponential phase, with a maximum at late exponential phase, and decreased gradually after entering the stationary phase (Fig. 6B) and that the expression level of *katE* stayed relatively low during the exponential phase and increased after entering the stationary phase (Fig. 6A). Thus, the expression of each catalase gene seemed to be elevated when the physiological demand became high. The increase of *katE* transcripts was confirmed by qRT-PCR, as described below.

We then analyzed the expression of the catalase gene in response to exogenous H_2O_2, because *katG* accompanied a putative *oxyR*-like transcriptional regulator gene with the locus tag mll6938 in the opposite direction. Although expression of the *katG-lacZ* fusion gene in aerobically grown exponential-phase cells showed no difference with or without H_2O_2 treatment, its expression increased approximately twofold in semiaerobically grown cells (data not shown). This increase indicated that our aerobic conditions induced *katG* expression. On the other hand, expression of *katE-lacZ* was almost unchanged under the conditions examined. The effects of H_2O_2 addition were also determined at the transcriptional level by qRT-PCR. The amount of *katG* transcripts increased approximately 3.7-fold upon addition of H_2O_2, but that of *katE* remained essentially unchanged (data not shown). The response to H_2O_2 was further confirmed by determining the catalase activities of cell extracts. The cellular catalase activities of MAFF303099 and ML2101D increased approximately 1.7-fold upon addition of H_2O_2, whereas that of ML6940DS was unchanged (Table 2). These results indicated that expression of *katG* was moderately controlled by exogenous H_2O_2.

Expression of *katE* and *katG* in planta. To investigate the expression of the two catalase genes during symbiotic interactions, we infected *L. japonicus* B-129 seedlings with MAFF303099 harboring either pKEZ01 or pKGZ01 and detected β-galactosidase activity by histochemical staining with X-Gal (Fig. 7). The rhizobial cells harboring pKGZ01 were strongly stained both inside the infection threads (Fig. 7C) and in infected nodule cells (Fig. 7F and I), indicating that *katG* expression continued at relatively high rates during and after establishing the infection process. In contrast, the cells harboring pKEZ01 were scarcely stained in infection threads (Fig. 7B) but stained moderately in infected nodule cells (Fig. 7E and H). Because this histochemical result showed elevated *katE* expression in the bacteroids, we investigated the transcript levels of the two catalase genes by qRT-PCR using *sigA*, encoding the σ^{70} protein, as a control. The relative expression rates of *katE* and *katG* in bacteroids were 4.4- and 0.6-fold higher, respectively, than those of free-living exponentially growing cells (Fig. 8). The increased expression rate of *katE* was also detected at stationary phase. The result also indicated that transcript levels of *katG* were at least 400 times higher than those of *katE* under all conditions examined.

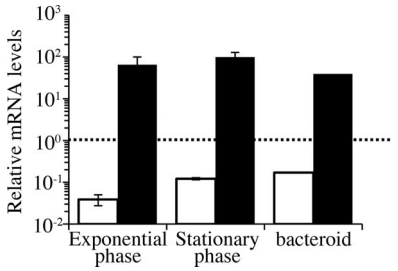

FIG. 8. Expression of catalase genes in free-living cells and bacteroids. The transcription levels of catalase genes were quantified by qRT-PCR using total-RNA samples as templates. The RNA samples were prepared from free-living aerobically grown exponential-phase (OD_{600} = 0.4) and stationary-phase (OD_{600} = 2.7) cells and bacteroids from 9-week-old nodules. The expression levels were normalized against the *sigA* gene as a standard. The open and closed bars indicate values for *katE* and *katG*, respectively. The values are means of three independent experiments with standard deviations.

DISCUSSION

The purpose of this work was to examine how *M. loti* MAFF303099 utilizes an assortment of catalases to survive and establish symbiotic nitrogen fixation. Through single and double gene disruption, together with expression analysis, we revealed that two catalases in *M. loti* MAFF303099, hereafter called $KatE_{Ml}$ and $KatG_{Ml}$, have distinct functions and that a lack of either of these catalases could not be reflexively compensated for by the other. The bifunctional catalase-peroxidase $KatG_{Ml}$ should play a major, if not a principal, role in the detoxification of internally generated H_2O_2, as well as a quasi-essential role in the detoxification of exogenous H_2O_2 at relatively high concentrations (approximately 60 μM or more), although the loss of $KatG_{Ml}$ scarcely affected nodulation and nitrogen fixation capacities. In contrast, the monofunctional catalase $KatE_{Ml}$ should have roles in optimizing survival during stationary phase and the capacity to fix nitrogen. Expression of $katG_{Ml}$ was highest at mid-exponential phase and was probably controlled to some extent by the accompanying *oxyR* homologue mll6938, whereas that of $katE_{Ml}$ was elevated during the stationary phase and under symbiotic nitrogen-fixing conditions and was not controlled by the *oxyR* homologue. The functional difference was partly explained by regulation of gene expression but might depend on intrinsic properties of the two enzymes.

The $katG_{Ml}$ mutant ML6940DS displayed elevated sensitivity to both endogenous and exogenous H_2O_2, and the expression of $katG_{Ml}$ was responsive to H_2O_2. These results indicate the importance of $KatG_{Ml}$ in H_2O_2 detoxification. Nevertheless, ML6940DS and the $katE_{Ml}$ $katG_{Ml}$ double mutant MLDKAT were still capable of proliferating under aerobic conditions with an approximately 50% longer generation time than the wild type. They could also survive or even proliferate in the presence of exogenous H_2O_2 at 60 μM or less (Fig. 3). Such an endurance capacity suggests that *M. loti* MAFF303099 has some system to detoxify H_2O_2 at a relatively low concentration other than the catalases, such as the alkyl hydroperoxide reductase (AhpC) of *E. coli*, which efficiently scavenges low levels of H_2O_2 (37). To encode such scavengers, *M. loti* possesses a number of potential genes with similarity to *E. coli ahpC* ($ahpC_{Ec}$), including mlr3745 and mll2432, though the similarity is limited (about 30%). Unlike that of *M. loti*, the bifunctional catalase gene $katG_{Bj}$ in *B. japonicum* USDA110 is almost essential for aerobic growth and probably functions to scavenge internally generated H_2O_2 (27). In addition, no double catalase mutant of $katA_{Sm}$ and $katB_{Sm}$ in *S. meliloti* Rm1021 has been obtained under aerobic conditions by standard mutagenesis procedures (15). These results indicate that different rhizobial species utilize different enzymes to dissipate low levels of H_2O_2 among rhizobial species.

It has been reported that H_2O_2, as well as superoxide, is generated by the host plants *Medicago sativa* and *Pisum sativum* at the early stage of rhizobial infection (34, 30). Furthermore, the $katA_{Sm}$ $katC_{Sm}$ double mutant of *S. meliloti* also has a defect in bacteroid formation, and the $katB_{Sm}$ $katC_{Sm}$ double mutant shows low nodulation efficiency and an inability to form bacteroids (15). These results support the deployment of H_2O_2 by host plants to control incoming rhizobial cells. Therefore, it is conceivable that *L. japonicus* produces a comparatively low level, if any, of H_2O_2 against infecting *M. loti* cells, because ML6940DS was vulnerable to external H_2O_2 at relatively high concentrations (60 μM or more) but still formed effective nodules like the wild type. Similar low-level H_2O_2 production might be expected for *P. vulgaris* when *R. etli* infects it (9).

The fact that the $katE_{Ml}$ mutant, ML2101D, lost colony-forming capacity earlier in stationary phase than the wild type (Fig. 4) suggests that $KatE_{Ml}$ participates in survival during the stationary phase. It might be reasonable for this physiological role that elevated expression of $katE_{Ml}$ was observed by both *lacZ* fusion and quantitative RT-PCR during stationary phase (Fig. 6 and 8). In contrast, $KatG_{Re}$ has been reported to function in both detoxification of exogenous H_2O_2 and survival in *R. etli* during the stationary phase (44). These results indicate that the physiological functions performed by the single catalase in *R. etli* are performed separately by the two enzymes in *M. loti*. This type of functional separation seems similar to that in *E. coli*, which has the sigma factor RpoS to control the expression of $katE_{Ec}$ during the stationary phase (32). However, *M. loti* and other *Rhizobium* species belonging to the *Alphaproteobacteria* lack *rpoS* homologues. It was recently reported for *S. meliloti* that an extracytoplasmic-function sigma factor encoded by the *rpoE2* gene controls the expression of *katC* and other genes during stationary phase (35). Although *M. loti* MAFF303099 possesses an *rpoE2* homologue, mll3697, how $katE_{Ml}$ is regulated by the mll3697 product remains unknown.

The $katE_{Ml}$ mutant ML2101D formed approximately 1.5-fold more nodules on *L. japonicus* but fixed nitrogen at rates of approximately 50 to 60% of those of wild-type nodules; in addition, the phenotype was complemented by transferring the plasmid containing $katE_{Ml}$. MLDKAT showed an essentially similar symbiotic phenotype. These results suggest that $KatE_{Ml}$ optimizes nitrogen fixation capacity. This decrease in nitrogen fixation capacity appears similar to those observed for the $katA_{Sm}$ $katC_{Sm}$ and $katB_{Sm}$ $katC_{Sm}$ double mutants, MK5003 and MK5004 (15, 39). However, the similarity is only superficial, because these mutants were less successful in nodulation and formed lower numbers of nodules with sparse or no bacteroids in contrast to ML2101D, which was fully successful in nodulation and formed a greater number of pink-red nodules.

The difference implies that ML2101D is defective in maintaining nitrogen fixation during stages later than the bacteroid formation stage, during and before which *S. meliloti* mutants seem to have defects. Although detailed morphological and biochemical investigations should be conducted on the nodule cells and bacteroids formed by ML2101D, the development of a greater number of nodules is a typical feature found in partially effective rhizobium-legume symbiosis between *L. japonicus* and *M. loti* (41, 21). The monofunctional catalase $KatE_{Ml}$ might scavenge not only H_2O_2 generated through the active aerobic respiration in bacteroids, but also H_2O_2 produced by senescing host cells, as reported for soybean nodules (1), or by sanction activity of host cells (19).

As discussed above, $KatE_{Ml}$ has specific roles in survival during the stationary phase and in the optimization of symbiotic nitrogen fixation. Its role in the latter function is particularly evident, because the mutants ML2101D and MLDKAT displayed practically identical symbiotic phenotypes. Substantial amounts of $KatG_{Ml}$ must be accumulated in stationary-phase cells and bacteroids, because the expression of $katG_{Ml}$ was at least 100 times higher than that of $katE_{Ml}$ under all the conditions investigated in this work. These results indicate that the functional separation between $KatE_{Ml}$ and $KatG_{Ml}$ is based on differences in biochemical properties, as well as differences in gene expression levels. There are two possibilities that include differences in affinity to H_2O_2 and dependency on pH or ionic conditions. The first possibility seems less likely, because homologues of $KatG_{Ml}$, such as $KatG_{Ec}$ and $KatB_{Sm}$, have nearly 100 times lower K_M values for H_2O_2 than homologues of $KatE_{Ml}$, such as $KatE_{Ec}$, $KatA_{Sm}$, and $KatC_{Sm}$ (24, 2). However, catalases do not follow standard Michaelis-Menten kinetics; thus, affinity values can be different under physiological conditions (for a review, see reference 6). Hence, the latter possibility seems more likely to fit the significance of monofunctional catalase $KatE_{Ml}$ under the physiological conditions, because the orthologous $KatC_{Sm}$ shows catalytic activity that is practically pH independent between pH 5 and 9 while the bifunctional catalase-peroxidase $KatB_{Sm}$ demonstrates a relatively sharp optimum around pH 6.5 (2). To understand the mechanism through which $KatE_{Ml}$ optimizes symbiotic nitrogen fixation, the two *M. loti* catalases must be further characterized.

ACKNOWLEDGMENTS

This work was supported in part by the Special Coordination Fund for Promoting Science and Technology and KAKENHI (Grant-in-Aid for Scientific Research) on Priority Areas "Comparative Genomics" from the Ministry of Education, Culture, Sports, Science and Technology of Japan.

We thank E. Mishima, E. Ishida, S. Okabe, and J. Maruya for the use of plasmids constructed in their unpublished works. We also thank the National BioResource Projects *Lotus* and *Glycine* at the Frontier Science Research Center, University of Miyazaki, Japan, for providing *L. japonicus* seeds.

REFERENCES

1. **Alesandrini, F., R. Mathis, G. Van de Sype, D. Hérouart, and A. Puppo.** 2003. Possible roles for a cysteine protease and hydrogen peroxide in soybean nodule development and senescence. New Phytol. **158:**131–138.
2. **Ardissone, S., P. Frendo, E. Laurenti, W. Jantschko, C. Obinger, A. Puppo, and R. P. Ferrari.** 2004. Purification and physical-chemical characterization of the three hydroperoxidases from the symbiotic bacterium *Sinorhizobium meliloti*. Biochemistry **43:**12692–12699.
3. **Bradford, M. M.** 1976. A rapid and sensitive method for the quantitation of microgram quantities of protein utilizing the principle of protein-dye binding. Anal. Biochem. **72:**248–254.
4. **Broughton, W. J., and M. J. Dilworth.** 1971. Control of leghemoglobin synthesis in snake beans. Biochem. J. **125:**1075–1080.
5. **Brown, S. M., M. L. Howell, M. L. Vasil, A. J. Anderson, and D. J. Hassett.** 1995. Cloning and characterization of the *katB* gene of *Pseudomonas aeruginosa* encoding a hydrogen peroxide-inducible catalase: purification of KatB, cellular localization, and demonstration that it is essential for optimal resistance to hydrogen peroxide. J. Bacteriol. **177:**6536–6544.
6. **Chelikani, P., I. Fita, and P. C. Loewen.** 2004. Diversity of structures and properties among catalases. Cell. Mol. Life Sci. **61:**192–208.
7. **Clare, D. A., M. N. Duong, D. Darr, F. Archibald, and I. Fridovich.** 1984. Effects of molecular oxygen on detection of superoxide radical with nitroblue tetrazolium and on activity stains for catalase. Anal. Biochem. **140:**532–537.
8. **Ditta, G., S. Stanfield, D. Corbin, and D. Helinski.** 1980. Broad host range DNA cloning system for gram-negative bacteria: construction of a gene bank of *Rhizobium meliloti*. Proc. Natl. Acad. Sci. USA **77:**7347–7351.
9. **Dombrecht, B., C. Heusdens, S. Beullens, C. Verreth, E. Mulkers, P. Proost, J. Vanderleyden, and J. Michiels.** 2005. Defence of *Rhizobium etli* bacteroids against oxidative stress involves a complexly regulated atypical 2-Cys peroxiredoxin. Mol. Microbiol. **55:**1207–1221.
10. **Hattori, Y., H. Omori, M. Hanyu, N. Kaseda, E. Mishima, T. Kaneko, S. Tabata, and K. Saeki.** 2002. Ordered cosmid library of the *Mesorhizobium loti* MAFF303099 genome for systematic gene disruption and complementation analysis. Plant Cell Physiol. **43:**1542–1557.
11. **Hérouart, D., S. Sigaud, S. Moreau, P. Frendo, D. Touati, and A. Puppo.** 1996. Cloning and characterization of the *katA* gene of *Rhizobium meliloti* encoding a hydrogen peroxide-inducible catalase. J. Bacteriol. **178:**6802–6809.
12. **Hirsch, A. M.** 1992. Developmental biology of legume nodulation. New Phytol. **122:**211–237.
13. **Imlay, J., A.** 2003. Pathways of oxidative damage. Annu. Rev. Microbiol. **57:**395–418.
14. **Jamet, A., E. Kiss, J. Batut, A. Puppo, and D. Hérouart.** 2005. The *katA* catalase gene is regulated by OxyR in both free-living and symbiotic *Sinorhizobium meliloti*. J. Bacteriol. **187:**376–381.
15. **Jamet, A., S. Sigaud, G. Van de Sype, A. Puppo, and D. Hérouart.** 2003. Expression of the bacterial catalase genes during *Sinorhizobium meliloti-Medicago sativa* symbiosis and their crucial role during the infection process. Mol. Plant-Microbe Interact. **16:**217–225.
16. **Jones, D. P.** 1982. Intracellular catalase function: analysis of the catalytic activity by product formation in isolated liver cells. Arch. Biochem. Biophys. **214:**806–814.
17. **Kaneko, T., Y. Nakamura, S. Sato, E. Asamizu, T. Kato, S. Sasamoto, A. Watanabe, K. Idesawa, A. Ishikawa, K. Kawashima, T. Kimura, Y. Kishida, C. Kiyokawa, M. Kohara, M. Matsumoto, A. Matsuno, Y. Mochizuki, S. Nakayama, N. Nakazaki, S. Shimpo, M. Sugimoto, C. Takeuchi, M. Yamada, and S. Tabata.** 2000. Complete genome structure of the nitrogen-fixing symbiotic bacterium *Mesorhizobium loti*. DNA Res. **7:**381–406.
18. **Kawano, M., T. Oshima, H. Kasai, and H. Mori.** 2002. Molecular characterization of long direct repeat (LDR) sequences expressing a stable mRNA encoding for a 35-amino-acid cell-killing peptide and a *cis*-encoded small antisense RNA in *Escherichia coli*. Mol. Microbiol. **45:**333–349.
19. **Kiers, E. T., R. A. Rousseau, S. A. West, and R. F. Denison.** 2003. Host sanctions and the legume-rhizobium mutualism. Nature **425:**78–81.
20. **Kouchi, H., K. Takane, R. B. So, J. K. Ladha, and P. M. Reddy.** 1999. Rice ENOD40: isolation, expression analysis in rice, transgenic soybean root nodules. Plant J. **18:**121–129.
21. **Krusell, L., K. Krause, T. Ott, G. Desbrosses, U. Kramer, S. Sato, Y. Nakamura, S. Tabata, E. K. James, N. Sandal, J. Stougaard, M. Kawaguchi, A. Miyamoto, N. Suganuma, and M. K. Udvardi.** 2005. The sulfate transporter SST1 is crucial for symbiotic nitrogen fixation in *Lotus japonicus* root nodules. Plant Cell **17:**1625–1636.
22. **Lange, R., and R. Hengge-Aronis.** 1991. Identification of a central regulator of stationary-phase gene expression in *Escherichia coli*. Mol. Microbiol. **5:**49–59.
23. **Livak, K. J., and T. D. Schmittgen.** 2001. Analysis of relative gene expression data using real-time quantitative PCR and the $2^{-\Delta\Delta}Ct$ method. Methods **25:**402–408.
24. **Loewen, P. C., and B. L. Triggs.** 1984. Genetic mapping of *katF*, a locus that with *katE* affects the synthesis of a second catalase species in *Escherichia coli*. J. Bacteriol. **160:**668–675.
25. **Miller, J. H.** 1972. Experiments in molecular genetics. Cold Spring Harbor Laboratory Press, Cold Spring Harbor, NY.
26. **Ohwada, T., Y. Shirakawa, M. Kusumoto, H. Masuda, and T. Sato.** 1999. Susceptibility of hydrogen peroxide and catalase activity of root nodule bacteria. Biosci. Biotechnol. Biochem. **63:**457–462.
27. **Panek, H. R., and M. R. O'Brian.** 2004. KatG is the primary detoxifier of hydrogen peroxide produced by aerobic metabolism in *Bradyrhizobium japonicum*. J. Bacteriol. **186:**7874–7880.
28. **Prapagdee, B., P. Vattanaviboon, and S. Mongkolsuk.** 2004. The role of a

bifunctional catalase-peroxidase KatA in protection of *Agrobacterium tumefaciens* from menadione toxicity. FEMS Microbiol. Lett. **232:**217–223.
29. **Prentki, P., and H. M. Krisch.** 1984. *In vitro* insertional mutagenesis with a selectable DNA fragment. Gene **29:**303–313.
30. **Rubio, M. C., E. K. James, M. R. Clemente, B. Bucciarelli, M. Fedorova, C. P. Vance, and M. Becana.** 2004. Localization of superoxide dismutases and hydrogen peroxide in legume root nodules. Mol. Plant-Microbe Interact. **17:**1294–1305.
31. **Saeki, K., K. Tokuda, T. Fujiwara, and H. Matsubara.** 1993. Nucleotide sequence and genetic analysis of the region essential for functional expression of the gene for ferredoxin I, *fdxN*, in *Rhodobacter capsulatus*: sharing of one upstream activator sequence in opposite directions by two operons related to nitrogen fixation. Plant Cell Physiol. **34:**185–199.
32. **Sak, B. D., A. Eisenstark, and D. Touati.** 1989. Exonuclease III and the catalase hydroperoxidase II in *Escherichia coli* are both regulated by the *katF* gene product. Proc. Natl. Acad. Sci. USA **86:**3271–3275.
33. **Sambrook, J., E. F. Fritsch, and T. Maniatis.** 1989. Molecular cloning: a laboratory manual, 2nd ed. Cold Spring Harbor Laboratory Press, Cold Spring Harbor, NY.
34. **Santos, R., D. Hérouart, S. Sigaud, D. Touati, and A. Puppo.** 2001. Oxidative burst in alfalfa-*Sinorhizobium meliloti* symbiotic interaction. Mol. Plant-Microbe Interact. **14:**86–89.
35. **Sauviac, L., H. Philippe, K. Phok, and C. Bruand.** 2007. An extracytoplasmic function sigma factor acts as a general stress response regulator in *Sinorhizobium meliloti*. J. Bacteriol. **189:**4204–4216.
36. **Schäfer, A., A. Tauch, W. Jäger, J. Kalinowski, G. Thierbach, and A. Pühler.** 1994. Small mobilizable multi-purpose cloning vectors derived from the *Escherichia coli* plasmids pK18 and pK19: selection of defined deletions in the chromosome of *Corynebacterium glutamicum*. Gene **145:**69–73.
37. **Seaver, L. C., and J. A. Imlay.** 2001. Alkyl hydroperoxide reductase is the primary scavenger of endogenous hydrogen peroxide in *Escherichia coli*. J. Bacteriol. **183:**7173–7181.
38. **Shaw, S. L., and S. R. Long.** 2003. Nod factor inhibition of reactive oxygen efflux in a host legume. Plant Physiol. **132:**2196–2204.
39. **Sigaud, S., V. Becquet, P. Frendo, A. Puppo, and D. Hérouart.** 1999. Differential regulation of two divergent *Sinorhizobium meliloti* genes for HPII-like catalases during free-living growth and protective role of both catalases during symbiosis. J. Bacteriol. **181:**2634–2639.
40. **Storz, G., L. A. Tartaglia, and B. N. Ames.** 1990. Transcriptional regulator of oxidative stress-inducible genes: direct activation by oxidation. Science **248:** 189–194.
41. **Suganuma, N., Y. Nakamura, M. Yamamoto, T. Ohta, H. Koiwa, S. Akao, and M. Kawaguchi.** 2003. The *Lotus japonicus* Sen1 gene controls rhizobial differentiation into nitrogen-fixing bacteroids in nodules. Mol. Genet. Genomics **269:**312–320.
42. **Triggs-Raine, B. L., B. W. Doble, M. R. Mulvey, P. A. Sorby, and P. C. Loewen.** 1988. Nucleotide sequence of *katG*, encoding catalase HPI of *Escherichia coli*. J. Bacteriol. **170:**4415–4419.
43. **Uchiumi, T., T. Ohwada, M. Itakura, H. Mitsui, N. Nukui, P. Dawadi, T. Kaneko, S. Tabata, T. Yokoyama, K. Tejima, K. Saeki, H. Omori, M. Hayashi, T. Maekawa, R. Sriprang, Y. Murooka, S. Tajima, K. Simomura, M. Nomura, A. Suzuki, Y. Shimoda, K. Sioya, M. Abe, and K. Minamisawa.** 2004. Expression islands clustered on the symbiosis island of the *Mesorhizobium loti* genome. J. Bacteriol. **186:**2439–2448.
44. **Vargas, M. C., S. Encarnacion, A. Davalos, A. Reyes-Perez, Y. Mora, A. Garcia-de los Santos, S. Brom, and J. Mora.** 2003. Only one catalase, KatG, is detectable in *Rhizobium etli*, and is encoded along with the regulator OxyR on a plasmid replicon. Microbiology **149:**1165–1176.
45. **von Ossowski, I., M. R. Mulvey, P. A. Leco, A. Borys, and P. C. Loewen.** 1991. Nucleotide sequence of *Escherichia coli katE*, which encodes catalase HPII. J. Bacteriol. **173:**514–520.
46. **Wayne, L. G., and G. A. Diaz.** 1986. A double staining method for differentiating between two classes of mycobacterial catalase in polyacrylamide electrophoresis gels. Anal. Biochem. **157:**89–92.